Separation Science and Technology
Publication details, including instructions for authors and subscription information:
http://www.informaworld.com/smpp/title~content=t713708471

Partial Oxidation of Methane in Permeable Ni Tube for Effective Hydrogen Production

Satoshi Fukada[a]; Shigeki Ono[a]
[a] Department of Advanced Energy Engineering Science, Kyushu University, Fukuoka, Japan

To cite this Article Fukada, Satoshi and Ono, Shigeki(2007) 'Partial Oxidation of Methane in Permeable Ni Tube for Effective Hydrogen Production', Separation Science and Technology, 42: 1, 73 — 87
To link to this Article: DOI: 10.1080/01496390600998078
URL: http://dx.doi.org/10.1080/01496390600998078

Separation Science and Technology, 42: 73–87, 2007

ISSN 0149-6395 print/1520-5754 online
DOI: 10.1080/01496390600998078

Partial Oxidation of Methane in Permeable Ni Tube for Effective Hydrogen Production

Satoshi Fukada and Shigeki Ono
Department of Advanced Energy Engineering Science,
Kyushu University, Fukuoka, Japan

Abstract: To develop an effective way to produce hydrogen continuously by means of partial oxidation of natural gas methane, we experimentally studied a Ni catalytic-permeable-membrane-tube reactor. When a mixture of CH_4 and O_2 was introduced into a Ni tube, H_2 was produced by a partial oxidation reaction and permeated through the Ni-tube reactor to separate from another product of CO. The dependence of the partial oxidation rate on the inlet CH_4/O_2 molar ratio, temperature, flow rate, and total pressure were determined experimentally. The rate constants of the complete oxidation reaction, the steam-reforming one and the CO_2-reforming one were simultaneously determined at temperatures of 400 to 750°C from fitting analytical calculations to experimental ones. Although complete separation between CO and H_2 was not achieved within a limited surface area in the present experiment, it was analytically proved that H_2 and CO can be effectively separated in a long Ni-tube reactor.

Keywords: Hydrogen, nickel, tubular reactor, partial oxidation, high-temperature gas-cooled reactor, natural gas, permeation

INTRODUCTION

Hydrogen is a promising secondary energy resource in the future. Hydrogen will be produced by means of solar energy battery or thermo-chemical decomposition of water using heat from high-temperature gas-cooled nuclear reactors (1). However, since the cost of solar battery and thermo-

Received 23 May 2006, Accepted 29 August 2006

Address correspondence to Satoshi Fukada, Department of Advanced Energy Engineering Science, Kyushu University, Fukuoka 812-8581, Japan. Tel.: 81-92-642-4140; Fax: 81-92-642-3783; E-mail: sfukada@nucl.kyushu-u.ac.jp

chemical decomposition to produce H_2 is high at present, the processes of steam reforming and partial oxidation of coal or natural gas have been utilized in hydrogen stations or hydrogen plants. In a conventional industrial partial oxidation system, e.g., the TEXACO system (2), H_2 is produced from coal, natural gas, and other hydrocarbons around at 1500°C without any catalyst. Since the reaction temperature is rather high, it wastes a large amount of usable heat. If we use an effective catalytic material for the partial oxidation process, the reaction temperature can be lowered down to around 700°C or temperatures still lower than it (3, 4).

There were many studies and industrial applications of a permeable membrane tube made of Pd alloys (5, 6) in order to purify or separate H_2 from gas mixtures. Although Pd is the most effective metal for the purpose of H_2 separation, its cost is high. Nickel is another possible permeable material for the H_2 separation, because the permeability of H atoms through Ni is also comparatively higher than other metals and is not sensitive to toxic gas such as CO. In addition to these advantages, Ni was considered the most effective catalyst material for the partial oxidation (4) and steam-reforming reactions. There were few studies that investigated Ni-tube reactors for the two purposes of H_2 production and separation (7). In the present study, a Ni catalytic-permeable-membrane-tube reactor is investigated for H_2 production by partial oxidation and for H_2 separation by means of the permeation of H atoms through Ni. Variations of the CH_4-to-H_2 conversion ratio with temperature, the inlet CH_4/O_2 molar ratio, gaseous velocity and total pressure are investigated experimentally and analytically.

EXPERIMENTAL

Figure 1 shows a schematic illustration of the experimental apparatus used in the present study. A mixture of CH_4 and O_2 controlled to a specified flow rate by two mass-flow meters was introduced into a permeable Ni tube from its top. The stated purity of the Ni tube used in the present study was 99%, and its impurity components were C 1000 ppm, Si 2200 ppm, Mn 2200 ppm, S 60 ppm, Cu 1500 ppm, Fe 2500 ppm, Mg 600 ppm. The Ni tube was 1000 mm in length, 3.18 mm in outside diameter, and 0.50 mm in thickness. The effective length of the Ni tube heated to a specified constant temperature was 700 mm. The outside tube was made of quartz glass of 778 mm in length and 9.5 mm in outside diameter. A constant flow rate of a $CH_4 + O_2$ gas mixture was supplied from the top of the Ni tube. At the same time, a constant flow rate of Ar was supplied from the bottom of a cylindrical space between the outside quartz tube and the inside Ni tube. The inside flow rate ranged from 10 to 100 cm^3(NTP)/min, and the outside one ranged from 10 to 200 cm^3(NTP)/min. The upstream flow rate was controlled by mass-flow meters, and the downstream flow rate was measured at the tube outlet by a soap-bubble flow meter. The heater in the electric furnace was

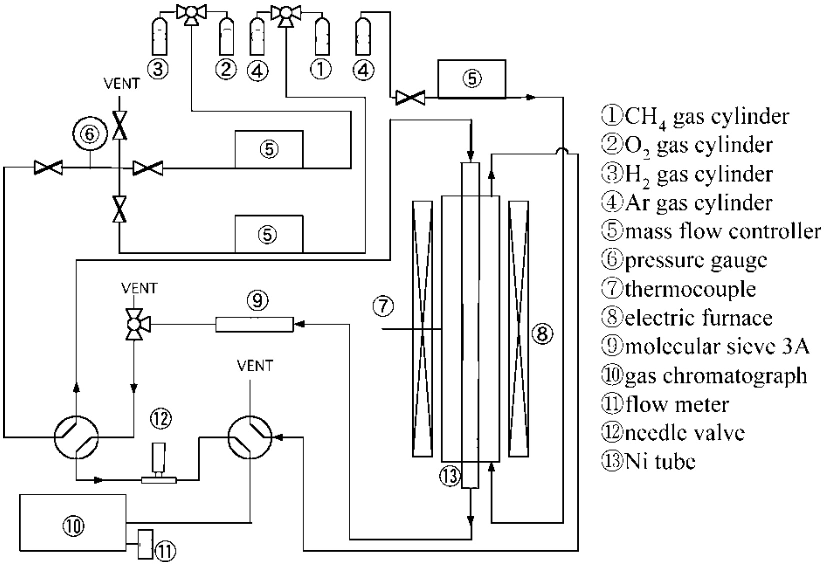

Figure 1. A schematic diagram of the experimental apparatus.

divided into four pieces, and respective electric currents were controlled to maintain a uniform temperature throughout the furnace. The temperature was measured by a thermocouple inserted into the tube. Temperature ranged from 400°C to 750°C. The total inlet pressure ranged from 1.0×10^5 Pa to 5.0×10^5 Pa.

A column packed with active alumina particles to remove water vapor produced by the partial oxidation process was inserted immediately after the Ni tube. The outlet concentrations of the gas mixture were measured by gas chromatography, and CH_4, O_2, H_2, CO, and CO_2 were detected. Any other trace-level gas components except for CH_4, O_2, H_2, CO, CO_2 and H_2O were not detected.

ANALYSIS

In the present experiment, a Ni catalytic-permeable-membrane tube is supplied with a mixture of CH_4 and O_2 under a constant flow rate and a constant temperature. Methane is partially oxidated on the Ni catalytic tube, and part of H_2 produced permeates through the Ni permeable tube.

The CH_4 oxidation reaction is described as follows:

$$CH_4 + 2O_2 \rightleftarrows CO_2 + 2H_2O \tag{1}$$

$$CH_4 + H_2O \rightleftarrows CO + 3H_2 \tag{2}$$

$$CH_4 + CO_2 \rightleftarrows 2CO + 2H_2 \tag{3}$$

The reactions of Eqs. (1–3) are generally called complete oxidation reaction, steam reforming one and CO_2 reforming one, respectively. Direct decomposition of CH_4 to $C + 2H_2$ on Ni surfaces (8) was not observed under the present O_2 rich condition. This is because the direct conversion occurred only under the condition of a very low O_2 concentration. Therefore, the direct decomposition process was not taken into consideration in the present study. The sum of the reactions. (1) – (3) leads to the following overall partial oxidation reaction:

$$CH_4 + (1/2)O_2 = CO + 2H_2 \tag{4}$$

Since the reaction (4) is not independent, it is not used for the present analytical calculation.

Two different reaction mechanisms were proposed for the partial oxidation process:

1. The reactions of Eq. (2) and Eq. (3) subsequent to Eq. (1) (9), and
2. a direct reaction pass described as $CH_4 + (1/2)O_2 \rightarrow C + 4H + O \rightarrow CO + H_2$ (3).

The reaction pass of (ii) may be valid only in the case of a small contact time on another transition metal catalyst. In the present Ni catalyst, the former process was considered predominant as would be proved later in the present paper. Therefore the second process was not taken into consideration in the present analysis.

The rates of the frontward and backward reactions (1)–(3) are defined as $r_{i,f}$ and $r_{i,b}$, $i = 1-3$, respectively. They are described in terms of the overall frontward reaction-rate constant $k_{i,f}$, as follows:

$$r_{1,f} = k_{1,f} p_{CH_4} p_{O_2}, \quad r_{1,b} = \frac{k_{1,f} p_{CO_2} p_{H_2O}^2}{K_1} \tag{5a, b}$$

$$r_{2,f} = k_{2,f} p_{CH_4} p_{H_2O}, \quad r_{2,b} = \frac{k_{2,f} p_{CO} p_{H_2}^3}{K_2} \tag{6a, b}$$

$$r_{3,f} = k_{3,f} p_{CH_4} p_{CO_2}, \quad r_{3,b} = \frac{k_{3,b} p_{CO}^2 p_{H_2}^2}{K_3} \tag{7a, b}$$

The order of the reaction rates of Eqs. (5ab)–(7ab), i.e., the index of each partial pressure is the same as ones assumed by Jim et al. (10). Different orders of reaction-rate equations were previously given to the CO_2-reforming reaction (11) or the steam-reforming reaction (12, 13). After some trial and error calculation, however, we found that the rate equations described above could reproduce our experimental data better.

The reaction-rate constant in the frontward direction, $k_{i,f}$, is correlated to the following Arrhenius equation:

$$k_{i,f} = k_{i,0} \exp\left(-\frac{E_i}{R_g T}\right) \quad \mathrm{i} = 1, 2, 3 \tag{8}$$

The values of the equilibrium constant appearing in Eqs. (5b)–(7b), K_i, are given by the Gibbs free-energy change, ΔG_i, in the thermodynamic table (14):

$$K_i = \exp\left(-\frac{\Delta G_i}{R_g T}\right) \quad \mathrm{i} = 1, 2, 3 \tag{9}$$

The differential material balance equations for respective molecular species of CH_4, O_2, H_2, H_2O, CO, and CO_2 are expressed in terms of each reaction rate, $r_{i,f}$ and $r_{i,b}$, as follows:

$$\frac{d}{dA}\left(W^{inside}\frac{p_{CH_4}}{p_t}\right) = -r_{1,f} + r_{1,b} - r_{2,f} + r_{2,b} - r_{3,f} + r_{3,b} \tag{10}$$

$$\frac{d}{dA}\left(W^{inside}\frac{p_{O_4}}{p_t}\right) = -2r_{1,f} + 2r_{1,b} \tag{11}$$

$$\frac{d}{dA}\left(W^{inside}\frac{p_{H_2}}{p_t}\right) = 3r_{2,f} - 3r_{2,b} + 2r_{3,f} - 2r_{3,b} - \frac{K_p}{2t}\Delta p_{H_2} \tag{12}$$

$$\frac{d}{dA}\left(W^{inside}\frac{p_{H_2O}}{p_t}\right) = 2r_{1,f} - 2r_{1,b} - r_{2,f} + r_{2,b} \tag{13}$$

$$\frac{d}{dA}\left(W^{inside}\frac{p_{CO}}{p_t}\right) = r_{2,f} - r_{2,b} + 2r_{3,f} - 2r_{3,b} \tag{14}$$

$$\frac{d}{dA}\left(W^{inside}\frac{p_{CO_2}}{p_t}\right) = r_{1,f} - r_{1,b} - r_{3,f} + r_{3,b} \tag{15}$$

In calculation, the increment of A was replaced by that of the distance from the Ni tube inlet in the axial direction, z. Therefore, $dA = \pi d dz$.

Since $p_t = p_{CH4} + p_{O2} + p_{H2} + p_{H2O} + p_{CO} + p_{CO2}$, the sum of the above mass-balance equations of Eqs. (10)–(15)can be reduced to the following equation:

$$\frac{dW^{inside}}{dA} = 2r_{2,f} - 2r_{2,b} + 2r_{3,f} - 2r_{3,b} - \frac{K_p}{2t}\Delta p_{H_2} \tag{16}$$

The last term of the right-hand side on Eq. (12) and Eq. (16) is the contribution of H_2 permeation through the Ni tube, where Δp_{H2} is the driving force of H_2 permeation that is different from place to place. In the present study the H_2 permeation is limited by diffusion through Ni. Therefore, Δp_{H2} was assumed to be equal to $(p_{H2}^{inside})^{0.5} - (p_{H2}^{outside})^{0.5}$.

When the Ni tube was supplied with a mixture of CH_4 and O_2 from the top, the concentration of each component at the inlet is given as follows:
at

$$z=0,\quad p_{CH_4}=p_{CH_4,in},\quad p_{O_2}=p_{O_2,in},\quad p_{CO_2}=p_{CO}=p_{H_2O}=p_{H_2}=0,$$
$$W^{inside}=W_0^{inside} \tag{17}$$

The seven ordinary differential equations, Eqs. (10), to (16), were simultaneously solved under the inlet condition of Eq. (17) by the Runge-Kutta method. The parameters that are determined experimentally are $k_{1,f}$, $k_{2,f}$ and $k_{3,f}$. A condition of the steady-state oxidation reaction and permeation was achieved around half an hour after the introduction of the gas mixture into the Ni tube reactor. Therefore we took only steady-state experimental data.

Before the above CH_4/O_2 supply experiment, the permeability of H atoms through the Ni tube used here was determined using an $Ar+H_2$ gas mixture. Figure 2 shows the experimental results. The permeability of H atoms through Ni, K_p, was correlated to the following equation:

$$K_P=4.99\times10^{-7}\exp\left(-\frac{51.9[\text{kJ/mol}-H]}{R_gT}\right)\ [\text{mol}-\text{H/msPa}^{0.5}] \tag{18}$$

The correlation is in close agreement with the best-fit equation that correlated more than 30 previous data by Robertson (15) as seen in the figure.

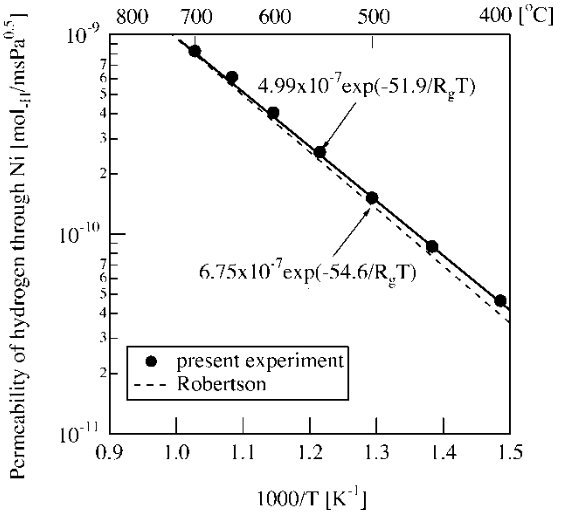

Figure 2. Permeability of hydrogen through Ni tube.

RESULTS AND DISCUSSION

Variations of $x_{j,out}$ with $x_{CH4,in}$ and T

Figure 3 shows variations of the outlet gas compositions, $x_{j,out}$, with the inlet CH_4 molar fraction, $x_{CH4,in}$, when different concentrations of the $CH_4 + O_2$ gas mixture were introduced into the tubular reactor. Gases detected were CH_4, O_2, H_2, H_2O, CO, and CO_2. Any other gaseous component was not detected throughout the present experiment. The total gas flow rate (10 cm^3(NTP)/min), W_o^{inside}, and the reactor temperature (700°C) were the same throughout the experiments in the figure.

Lines in the figure are calculation results determined using the ordinary differential equations given in the preceding chapter. The results depicted by a solid line and open circles are the sum of the outlet H_2 concentrations in the inside (i.e. non-permeated part) and the outside (i.e. permeated part) of the Ni tube. As expected, the complete oxidation was predominant under the lower CH_4 concentration region of $x_{CH4,in} < 0.4$. For example, the main components at the outlet when $x_{CH4,in} = 0.3$ were CO_2 and H_2O, and $x_{H2,out}$ and $x_{CO,out}$ were very small. The outlet molar fractions of H_2 and CO increased with the increase of $x_{CH4,in}$. These results indicate that the two-step reaction is predominant in the Ni-tube reactor: In the first step, the complete oxidation reaction of Eq. (1) proceeds, and in the second step remaining CH_4 reacts with the reaction products of CO_2 and H_2O as shown in Eqs. (2) and (3). We found that the optimum inlet condition for partial oxidation to give the maximum $x_{H2,out}$ value is $x_{CH4,in}/x_{O2,in} = 2$. In the

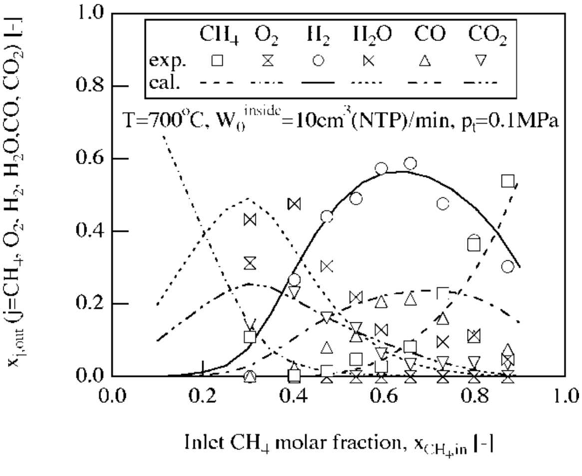

Figure 3. Variations of outlet molar fraction of each component with different inlet CH_4 concentrations.

following paragraphs, we focus on experiments under the optimum inlet condition of $CH_4 + O_2$ (2:1) feed.

Figure 4 shows a comparison of the molar fraction of each component at the Ni tube outlet between experiment and calculation for different temperatures from 400 to 750°C. A comparatively close agreement was obtained between the experiment and the calculation regardless of different temperatures. As seen in the figure, the values of $x_{H2,out}$ and $x_{CO,out}$ when $T < 550°C$ were very small. There was no H_2 production under temperatures lower than 550°C. Thus, the complete oxidation of the reaction (1) was predominant when $T < 550°C$ similarly to our previous study (4). This is because the equilibrium constants of K_2 and K_3 of Eq. (9) were very small in the lower temperature region. On the contrary, the H_2 production by partial oxidation of the reaction (4) became predominant under temperatures higher than 600°C. The calculation is in good agreement with the experimental behavior of H_2 production even at any temperature.

CH_4-to-H_2 Conversion Ratio and CO Selectivity with Inlet Flow Rate and Total Pressure

Figure 5 shows variations of the CH_4-to-H_2 conversion ratio with the inside gas flow rate at three different temperatures when the optimum concentration of $CH_4 + O_2$ (2 : 1) gas mixture was introduced into the Ni

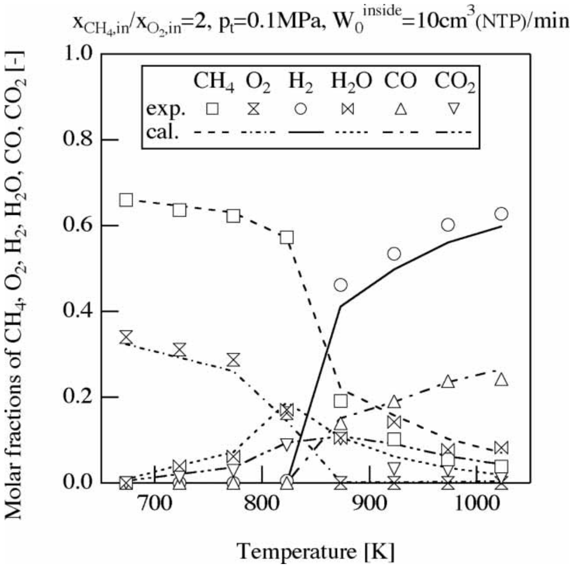

Figure 4. Variations of outlet molar fraction of each component with different temperatures.

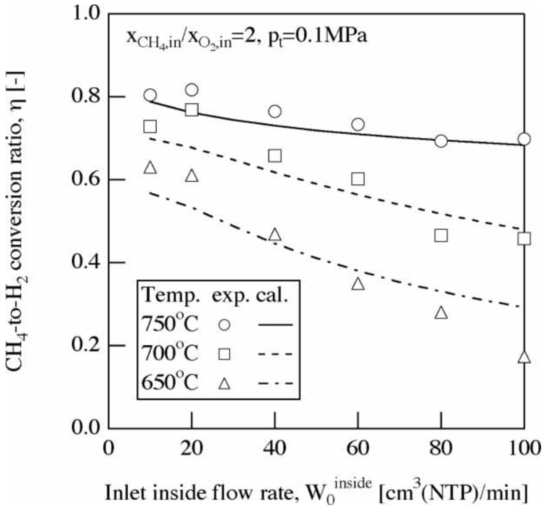

Figure 5. CH_4-to-H_2 conversion ratio as a function of total inlet flow rate and temperature.

catalytic-permeable-membrane tube. The CH_4-to-H_2 conversion ratio denoted by η on the vertical axis means the ratio of the H_2 production rate to the molar rate of hydrogen supplied as CH_4 and is defined as follows:

$$\eta = \frac{W_{out}^{inside} x_{H_2,out}^{inside} + W_{out}^{outside} x_{H_2,out}^{outside}}{2W_0^{inside} x_{CH_4,in}} \tag{19}$$

Here, the first term on the numerator of the right-hand side of Eq. (19) is the part of non-permeated H_2 and the second term is the permeated part. As seen in Fig. 5, η varied with W_0^{inside}. In other words, the CH_4-to-H_2 conversion ratio was a function of contact time when a gas mixture flowed through the Ni tube. The conversion ratio of η increased with an elevation of temperature or a decrease of the inlet inside flow rate. Lines in the figure show the numerical simulation based on the present rate-equation model of Eqs. (5) to (17). Regardless of different temperatures and flow rates, the numerical results predicted well the experimental results of the CH_4-to-H_2 conversion ratio. The maximum η value obtained in the present study was 0.82.

Figure 6 shows the CH_4-to-H_2 conversion ratio and the CO selectivity as a function of the inlet total pressure, p_t. The CO selectivity, S_{CO}, is defined as follows:

$$S_{CO} = \frac{x_{CO,out}}{x_{CO,out} + x_{CO_2,out}} \tag{20}$$

As seen in Fig. 6, η decreased with the increase of p_t. This is because the total gas amount increases in the right direction of the reaction (4). The overall

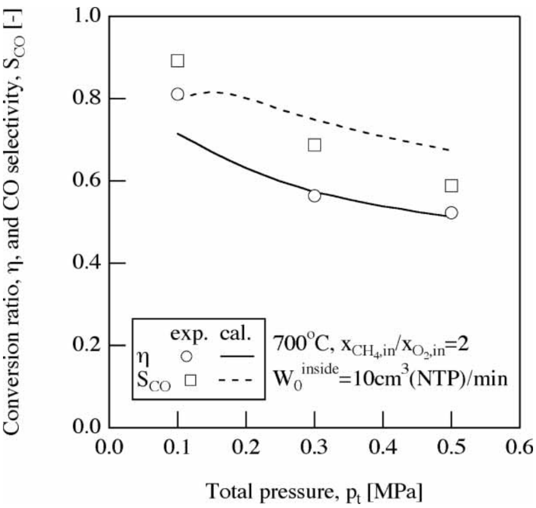

Figure 6. CH_4-to-H_2 conversion ratio and CO selectivity as a function of total inlet pressure.

behavior of the CH_4-to-H_2 conversion was also predicted well by the numerical simulation. The CO selectivity of S_{CO} also behaves in a similar way to η. Thus, we can expect a high efficiency of a Ni catalytic-permeable-membrane-tube reactor for the simultaneous production of H_2 and CO from CH_4.

H_2 Permeation Rate as a Function of Outside Flow Rate and Total Pressure

Figure 7 shows that the overall H_2 permeation rates, $W_{out}^{outside}x_{H2,out}$, are almost independent of the inlet outside Ar flow rate, $W_0^{outside}$. The line of the H_2 permeation rate is calculated by the following equation for the diffusion-limiting permeation condition:

$$W_{out}^{outside}x_{H_2,out}^{outside} = \int_{inlet}^{outlet} \frac{K_P}{2t} \times \left\{(p_t^{inside}x_{H_2}^{inside})^{0.5} - (p_t^{outside}x_{H_2}^{outside})^{0.5}\right\}\pi d dz \quad (21)$$

Close agreement is obtained between experiment and calculation. The fact means that the intrinsic H_2 permeability is independent of the inside flow condition and the CO and CO_2 concentrations. Therefore, we concluded that the rate-determining step of H_2 permeation is diffusion of H atom through Ni.

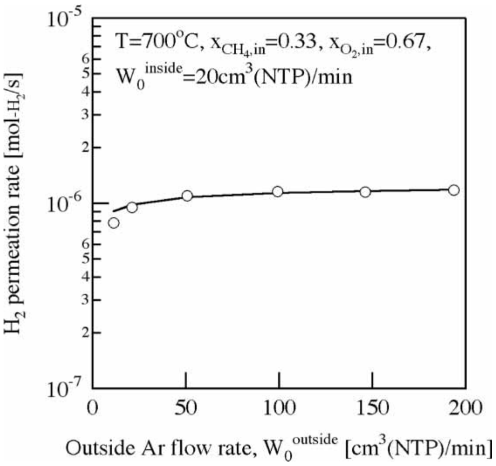

Figure 7. Overall H_2 permeation rate as a function of outside Ar flow rate.

Figure 8 is a graph showing what fraction of H_2 produced in the Ni catalytic tubular reactor permeates through the Ni permeable tube. The fraction denoted by ζ is defined as follows:

$$\zeta = \frac{W^{outside} x^{outside}_{H_2,out}}{W^{inside}_{out} x^{inside}_{H_2,out} + W^{outside}_{out} x^{outside}_{H_2,out}} \tag{22}$$

The fraction $\zeta$was not so high under the condition of 0.1 MPa $CH_4 + O_2$ gas supply. However, the fraction increased with the total pressure, p_t. This is

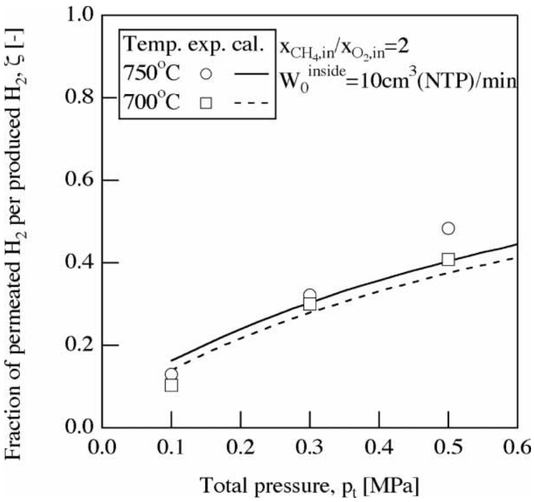

Figure 8. Fraction of permeated H_2 to its amount produced in Ni tube.

because the driving force of permeation, Δp_{H2}, increased. The calculation results are also comparatively in good agreement with the experimental data. The value of the H_2 permeability used for the calculation was the same one, Eq. (18), determined under the condition without any toxic gas such as CO. Therefore, we can say that not only the feed components of CH_4 and O_2 but also the by-products of CO, CO_2 and H_2O etc. had no effect on the permeability of H atoms through Ni at all.

Since η decreased with p_t as seen in Fig. 6, and ζ increased with p_t as seen in Fig. 8, there seems to be the optimum pressure condition in applications of the Ni-tube system to industrial hydrogen production and separation processes. Figure 9 shows variations of a product of η and ζ as a function of p_t. The product means the rate of H_2 permeated per that of CH_4 supplied. As seen in Fig. 9, the maximum fraction $\eta\zeta$ of the H_2 amount separated from CO using the Ni tube of 70 cm in length was 0.33 at $T = 750$ °C and $p_t = 5$ MPa. The value seems not to be sufficient for industrial application. Therefore, we need to use a thinner Ni membrane or a longer Ni tube in order to enhance the permeation rate of H_2 through Ni. This will be done in the future study.

Strictly saying, the incomplete separation arises from the H_2 permeability of Ni being lower than that of Pd. The permeability of H atoms through Ni ($K_P = 8.24 \times 10^{-10}$ mol-H/msPa$^{0.5}$ at 700°C) is smaller than one-hundredth of that of Pd ($K_P = 2.06 \times 10^{-7}$ mol-H/msPa$^{0.5}$) (16), which has the largest permeability among the all metals. Two chain lines in Fig. 9 show calculation results of the product $\eta\zeta$ if the permeability of the tube

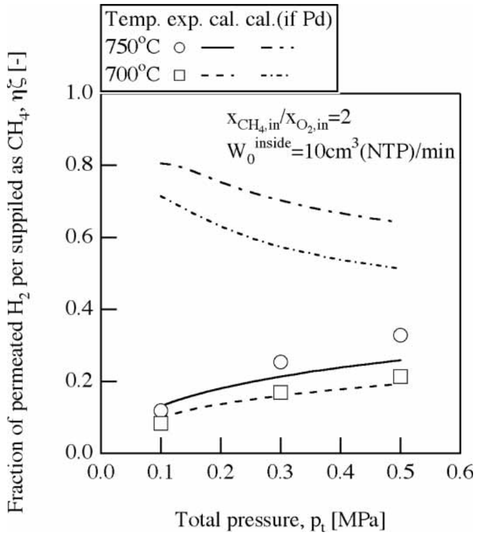

Figure 9. Fraction of permeated H_2 to supplied CH_4 as a function of total pressure.

wall is assumed to be the same as that of Pd with holding partial oxidation reaction rates of Ni. The system can be realized only under an ideal condition where H_2 produced by partial oxidation permeates to the outside flow without delay. The system requires the condition where CO or other reaction products do not degrade the permeability of Pd and the partial oxidation proceeds on Ni catalyst efficiently. This experimental proof will be done also in the future study.

Reaction Rate Constants as a Function of Temperature

Figure 10 shows variations of the three rate constants with the reciprocal of temperature. They were correlated to a unique function of temperature. Each rate constant is expressed by the following Arrhenius equations:

$$k_{1,f} = 7.27 \times 10^{4} \exp\left(-\frac{114[\mathrm{kJ/mol}]}{R_g T}\right) \quad [\mathrm{mol/m^2 atm^3}] \tag{23}$$

$$k_{2,f} = 4.68 \times 10^{7} \exp\left(-\frac{181[\mathrm{kJ/mol}]}{R_g T}\right) \quad [\mathrm{mol/m^2 atm^2}] \tag{24}$$

$$k_{3,f} = 3.04 \times 10^{15} \exp\left(-\frac{304[\mathrm{kJ/mol}]}{R_g T}\right) \quad [\mathrm{mol/m^2 atm^2}] \tag{25}$$

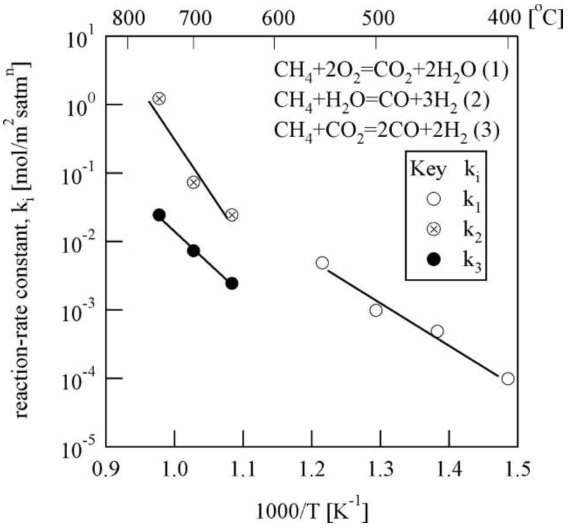

Figure 10. Variations of three reaction-rate constants with the reciprocal of temperature.

CONCLUSIONS

A catalytic-permeable-membrane tube made of Ni was studied for effective H_2 production based on partial oxidation and hydrogen permeation. With the optimum supply condition of a gas mixture of $CH_4/O_2 = 2$, H_2 and CO were produced by partial oxidation, and only H_2 permeated through the Ni tube with high efficiency without any toxic effect by CO. The maximum CH_4-to-H_2 conversion ratio was 0.82 and the maximum fraction of H_2 permeation was 0.48 for a 70 cm Ni tube system. The dependences of the rate constants of partial oxidation and permeation on the inlet CH_4/O_2 molar ratio, temperature, inside and outside flow rates, and total pressure were clarified. Their experimental behavior was simulated well by the three rate constants of complete oxidation, steam-reforming, and CO_2-reforming reactions.

NOMENCLATURE

A	inside surface area of Ni tube, m^2
d	diameter of Ni tube, m
E	activation energy of reaction, J/mol
$k_{i,f}$	frontward rate constant of reaction i ($i = 1-3$), mol/m^2sPa^n
K_i	equilibrium constant of reaction i ($i = 1-3$), Pa^n
K_p	permeability of hydrogen through Ni, mol-H/$msPa^{0.5}$
n	order of reaction
p_j	partial pressure of component j ($j = CH_4, O_2, H_2, H_2O$, CO and CO_2), Pa
p_0	atmospheric pressure, Pa
p_t	total pressure, Pa
R_g	gas law constant, kJ/molK
$r_{i,b}$	backward rate of reaction i ($i = 1-3$), $mol/m^2sPa^{n'}$
$r_{i,f}$	frontward rate of reaction i ($i = 1-3$), $mol/m^2sPa^{n'}$
S_{CO}	CO selectivity defined as Eq. (20)
t	thickness of Ni tube, m
W	total molar flow rate, mol/s or cm^3(NTP)/min
W^{inside}	outlet molar flow rate inside Ni tube, mol/s
$W^{outside}$	outlet molar flow rate outside Ni tube, mol/s
W_0^{inside}	inlet total molar rate of inside flow, mol/s or cm^3(NTP)/min
x_j	molar fraction of component j ($j = CH_4, O_2, H_2, H_2O$, CO and CO_2)
z	axial distance, m
$\Delta\Gamma_i$	Gibbs free-energy change of reaction i ($i = 1-3$), J/molK
Δp_{H2}	driving force of hydrogen permeation, Pa
η	CH_4-to-H_2 conversion ratio defined as Eq. (19)
ζ	fraction of permeated H_2 to produced H_2 in Ni tube defined as Eq. (22)

REFERENCES

1. Ohashi, H., Inaba, Y., and Nishihara, T. *et al*. (2004) Performance test results of mock-up facility of HTTR hydrogen production system. *J. Nucl. Sci. Technol.*, 41: 385–392.
2. Steimberg, M. and Cheng, H.C. (1989) Modern and prospective technologies for hydrogen production from fossil fuels. *Int. J. Hydrogen Energy.*, 14: 797–820.
3. Ashcroft, A., Cheethman, A., and Floord, J.S. *et al*. (1990) Selective oxidation of methane to synthesis gas using transition metal catalyst. *Nature*, 344: 319–321.
4. Fukada, S., Nakamura, N., and Monden, J. (2004) Effects of temperature, oxygen-to-methane molar ratio and superficial gas velocity on partial oxidation of methane for hydrogen production. *Int. J. Hydrogen Energy*, 29: 619–625.
5. Wang, D., Flanagan, T.B., and Shanahan, K.L. (2004) Permeation of hydrogen through pre-oxidized Pd membranes in the presence and absence of CO. *J. Alloys Comp.*, 372: 158–164.
6. Yamakawa, K., Ege, M., Ludescher, B., and Hirscher, M. (2003) Surface adsorbed atoms suppressing hydrogen permeation of Pd membranes. *J. Alloys Comp.*, 352: 57–59.
7. Bustamante, F., Enick, R.M., and Cugini, A.V. *et al.* (2004) High-temperature kinetics of the homogeneous reverse water-gas shift reaction. *AIChE J.*, 50: 1028–1041.
8. Fukada, S., Nakamura, N., Monden, J., and Nishikawa, M. (2004) Experimental study of cracking methane by Ni/SiO_2 catalyst. *J. Nucl. Mater.*, 329–333: 1365–1369.
9. Prettre, M., Eichner, C., and Perrin, M. (1946) *Trans. Faraday Soc.*, 43: 335–340.
10. Jin, W., Gu, X., and Li, S. *et al.* (2000) Experimental and simulation study on a catalyst packed tubular dense membrane reactor for partial oxidation of methane to syngas. *Chem. Eng. Sci.*, 55: 2617–2625.
11. Wang, S. and Lu, G.Q. (1999) A comprehensive study on carbon dioxide reforming of methane over $Ni/\gamma\text{-}Al_2O_3$ catalysts. *Ind. Eng. Chem.*, 38: 2615–2625.
12. Xu, J. and Fromen, G.F. (1990) Methane steam reforming, methanation and water-gas shift. *AIChE J.*, 45: 491–501.
13. Gunn, D.J. (2004) Production of hydrogen-rich gases from steam reforming of methane in an automatic catalytic microreactor. *Int. J. Hydrogen Energy*, 29: 1427–1428.
14. Kubaschewski, O. and Alcock, C.E. (1979) *Metallurgical Thermochemistry*, 5th ed.; Pergamon Press: New York.
15. Robertson, W.M. (1973) Hydrogen permeation, diffusion and solution in nickel. *Z. Metallkunde*, 64: 436–443.
16. Lasser, R. (1989) *Tritium and Helium-3 in Metals*; Springer-Verlag: Berlin.